Available online at www.sciencedirect.com
SCIENCE DIRECT®
Journal of Molecular Catalysis A: Chemical 224 (2004) 197–205
JOURNAL OF MOLECULAR CATALYSIS A: CHEMICAL
www.elsevier.com/locate/molcata

The role of positively charged meso-substituents on the kinetics of the reductive nitrosylation of iron(III)-porphyrins The catalytic role of nitrite

Alexander Theodoridis, Rudi van Eldik*

Institute for Inorganic Chemistry, University of Erlangen-Nürnberg, Egerlandstrasse 1, 91058 Erlangen, Germany

Abstract

The reaction of $[Fe^{III}(TMPyP)(H_2O)_2]^{5+}$, TMPyP = meso-tetra-*N*-methyl-pyridyl-porphine, with NO to form $[Fe^{II}(TMPyP)(NO^+)(H_2O)]^{5+}$ was studied at pH = 1. Stopped-flow techniques were employed to study the reversible binding reaction of NO as a function of concentration, temperature and pressure. The reverse release of NO was studied directly by using $[Fe(H_2O)_6]^{2+}$ as a scavenger for NO as a function of temperature and pressure. The reported activation parameters, especially the positive activation entropy and volume values, favour the operation of a dissociative interchange (I_d) mechanism. A volume profile for the overall reaction is reported, and the results are discussed in terms of the influence of the positively charged substituents on the porphyrin chelate. The reaction of the product, $[Fe^{II}(TMPyP)(NO^+)(H_2O)]^{5+}$, with NO_2^- was studied at pH = 4 under pseudo-first-order conditions. Concentration, temperature and pressure dependencies of the reaction were investigated. Possible mechanisms for the nitrite catalyzed reductive nitrosylation reaction are presented.

Keywords: Reductive nitrosylation; Nitrite catalysis; Fe-porphyrin complexes

1. Introduction

NO plays an important role in mammalian biology. It controls the blood pressure and is responsible for the activation of guanylate cyclase [1]. It also functions as an inhibitor of cytochrome *c* oxidase [2]. Its reactions with heme systems like hemoglobin, met-hemoglobin [3], cytochrome c^{II} [4], and cytochrome P450 and $P450_{cam}$ [5], have been extensively studied thermodynamically and kinetically. However, in these systems the morphology of the metal environment (protein, different substituents, charge, etc.) plays an important role in the rate of the reaction, as well as in the nature of the reaction products and underlying reaction mechanism. In the case of cytochrome P450 and $P450_{cam}$ for example [5], it was found that cytochrome $P450_{cam}$ reacts faster with NO than the enzyme in the absence of camphor. It is also known that Fe(III)-porphyrins react several orders of magnitude faster with NO than other Fe(III) complexes in acidic media [6]. In fact, $Fe^{III}(edta)H_2O$ does not react with NO at all, whereas the corresponding $Fe^{II}(edta)H_2O$ complex is an excellent NO scavenger [7]. The characteristic reactivity of Fe(III)-porphyrins has led to an increasing interest in this chemistry over the past years. Speciation as a function of pH, redox potentials, ligand substitution reactions and water exchange reactions have been studied in order to understand the underlying reaction mechanisms [8–10]. Important at this point is that different meso-substituents lead to significant differences in the rate of the substitution reactions and in the pK_a values of the coordinated water molecules.

Model systems studied are the porphyrins $[Fe^{III}(TPPS)(H_2O)_2]^{3-}$, $[Fe^{III}(TMPS)(H_2O)_2]^{3-}$ and $[Fe^{III}(TMPyP)(H_2O)_2]^{5+}$, which are presented schematically in Fig. 1 (TPPS = tetraphenylporphinato-4-sulfonate, TMPS = tetramesitylporphinato-4-sulfonate, TMPyP = tetra-4-methylenpyridyl-porphine). These Fe(III)-porphyrins differ in two aspects: steric hindrance at the porphyrin (FeTPPS and FeTMPS), and overall charge (FeTPPS and FeTMPyP). There is no other effect (for example protein environment) that could complicate the kinetic behavior of these systems.

* Corresponding author. Tel.: +49 9131 857350; fax: +49 9131 857387.
E-mail address: vaneldik@chemie.uni-erlangen.de (R. van Eldik).

1381-1169/$ – see front matter © 2004 Elsevier B.V. All rights reserved.
doi:10.1016/j.molcata.2004.09.021

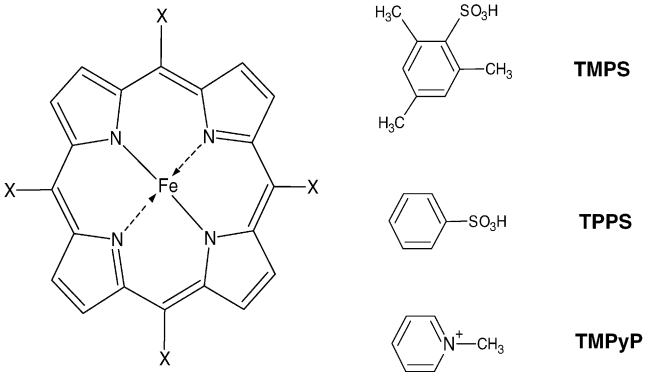

Fig. 1. The three model porphyrins. The water molecules, which are axially coordinated at the iron center, are not shown. The sulfonato groups on Fe(TMPS) and Fe(TPPS) are deprotonated in aqueous solution.

In this study we investigated the effect of the positive charge on the porphyrin in $[Fe^{III}(TMPyP)(H_2O)_2]^{5+}$ on its substitution behavior. Laverman and Ford [6] studied the reactions of the above-mentioned anionic porphyrin complexes with NO. In the present study the interaction of NO in acidic media with the third complex, viz. $[Fe^{III}(TMPyP)(H_2O)_2]^{5+}$, was investigated. A comparison with the data for the other anionic porphyrin complexes [6], as well as with water exchange data for all three systems [11], is presented. The reaction was also studied at pH = 4 where nitrite acts as a catalyst for the reductive nitrosylation process. Nitrite can play an important catalytic role in these reactions especially at higher pH. The mechanistic clarification of this process is of fundamental interest to nitrosylation processes in biological systems [12].

2. Experimental

2.1. Chemicals

Doubly distilled water was used for the preparation of all solutions. All chemicals used were of analytical grade. $[Fe^{III}(TMPyP)(H_2O)(OH)](Tos)_4$ was purchased from Frontier Scientific Ltd. Fine Chemicals, Utah, USA, and was used without further purification. NO was obtained from Air Liquide. It was purified by passing through a double column of Ascarite II (NaOH on silica gel, Aldrich), to avoid traces of nitrite in the aqueous solutions of NO, and through phosphorpentoxide (Fluka). Trifluoromethanesulfonic acid (CF_3SO_3H) obtained from Acros Organics, was used to prepare solutions of the diaqua complex at pH = 1. $NaNO_2$ was obtained from Merck and lithiumtriflate from Aldrich.

2.2. Solution preparation

All solutions and buffers were firstly deoxygenated with argon or nitrogen, and then saturated with NO. Since the NO concentrations could not be measured directly the concentration of diluted solutions was measured (see below), and the initial NO concentration was then extrapolated. Solutions of lower concentrations were prepared by diluting saturated NO solutions with 0.1 M triflic acid. All NO solutions were freshly prepared and used within a few hours.

The reaction of $[Fe^{II}(TMPyP)(H_2O)(NO^+)]^{5+}$ (obtained as product in the reaction of the diaqua complex with NO) with nitrite was studied in acetate buffer (acetic acid/sodium acetate) with an ionic strength of 0.1 M and a pH of 4.0. The buffer concentration was 0.02 M, and the ionic strength was adjusted by addition of lithiumtriflate. Complex solutions were prepared by dissolving a weighed amount of the complex in the buffer solution. The NO/NO_2^- solutions were prepared by first degassing and then saturating the NO_2^- solutions with NO, which were prepared by weighing the calculated amount of nitrite into the buffer.

2.3. Instrumentation

The determination of the concentration of NO in all solutions was performed with an ISO-NOP electrode connected to an ISO-NO Mark II nitric oxide sensor from World Precision Instruments Inc. The NO electrode was calibrated with fresh solutions of sodium nitrite and potassium iodide according to the method suggested by the manufacturers. The calibration factor nA/μM was determined with a linear fit program. UV–vis spectra were recorded on Varian Cary 1G and Cary 5G spectrophotometers. A Metrohm 702 SM Titrino was used for the spectrophotometric titrations. Stopped-flow measurements were performed on an SX-18 MV stopped-flow spectrophotometer from Applied Photophysics. The circulator water used for temperature control of the instrument was in all cases saturated with nitrogen. Deoxygenated solutions of Fe(TMPyP) were rapidly mixed with NO solutions of different concentrations. Kinetic traces were monitored at 424 nm and analyzed by the SX-18 MV program for a single exponential fit of the data. Rapid scan measurements were performed on the same instrument by connecting it to a J&M rapid scan detector, attached to a TIDAS 16-416 spectrophotometer. The spectra were imported into the SPECFIT program and analyzed.

High-pressure stopped-flow experiments were performed on a custom-built instrument described previously [13,14] at pressures up to 130 MPa. The kinetic traces were recorded at 424 nm on an IBM-compatible PC and analyzed with the OLIS KINFIT (Bogart, GA, 1989) set of programs.

All kinetic measurements were performed under pseudo-first-order conditions, i.e. with at least a 10-fold excess of NO or nitrite. The kinetic trace was monitored until there were no further absorbance changes in the UV–vis spectra. The reported rate constants represent the mean values of between 5 and 8 kinetic traces.

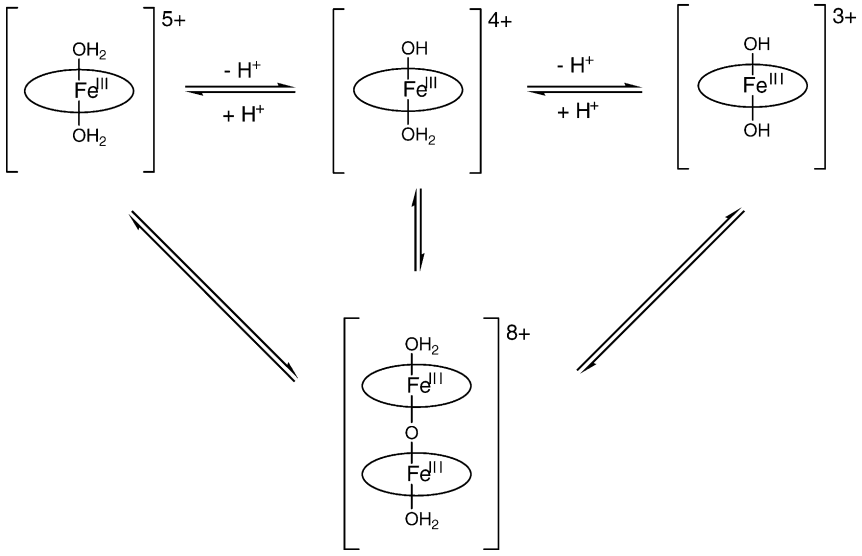

Scheme 1. Deprotonation of the $[Fe^{III}(TMPyP)(H_2O)_2]^{5+}$ complex and its dimerization.

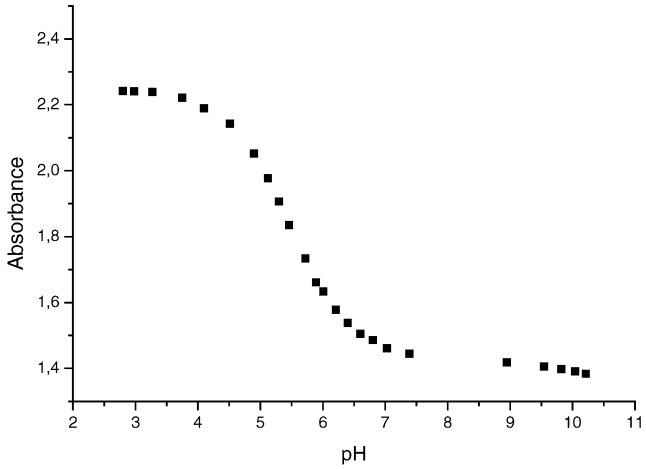

Fig. 2. Absorbance of $[Fe^{III}(TMPyP)(H_2O)_2]^{5+}$ at 400 nm as a function of pH.

3. Results and discussion

It was essential to determine the speciation of the Fe^{III}(TMPyP) complex as a function of pH. It is well known that such porphyrin complexes exhibit equilibria between aqua, hydroxo and μ-oxo-dimeric forms as shown in Scheme 1. The absorbance changes at 400 nm as a function of pH (Fig. 2) clearly show that below pH = 3 only the fully protonated $[Fe^{III}(TMPyP)(H_2O)_2]^{5+}$ species is present in solution. When the points are fitted to a single sigmoidal function, the calculated value of the first pK_a is 5.49 ± 0.02, which is in good agreement with literature data for this complex (viz. 5.5 ± 0.2) [15–18]. By way of exception, one other study [19] reported a pK_a value of 4.7 for $[Fe^{III}(TMPyP)(H_2O)_2]^{5+}$. Laverman [20] also determined the pK_a value of $[Fe(TMPS)(H_2O)_2]^{3-}$ by the same method and reported a value of 7.6. The significantly lower pK_a value found for the $[Fe^{III}(TMPyP)(H_2O)_2]^{5+}$ complex as compared to those for the anionic complexes can easily be accounted for in terms of the high positive charge that will induce deprotonation of the coordinated water molecules. The second pK_a value must be significantly higher and is not of interest for the present study.

On the basis of the lower pK_a value for $[Fe^{III}(TMPyP)(H_2O)_2]^{5+}$, it was necessary to work at a lower pH to ensure that we are mainly dealing with the reactions of the diaqua complex and not with that of the aqua-hydroxo or even the dimeric μ-oxo-bridged complex. Since it is known that Fe-porphyrins decompose in acidic media, freshly prepared solutions of the investigated complex were studied over longer periods of time and showed no UV–vis spectral changes over 2–3 days.

3.1. UV–vis observations and kinetics of the binding of NO to $[Fe^{III}(TMPyP)(H_2O)_2)]^{5+}$

The reaction of $[Fe^{III}(TMPyP)(H_2O)_2]^{5+}$ with NO is a second-order process as shown in Scheme 2, and is expected

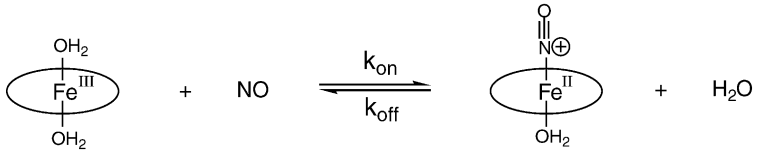

Scheme 2. The reaction of $[Fe^{III}(TMPyP)(H_2O)_2]^{5+}$ with NO.

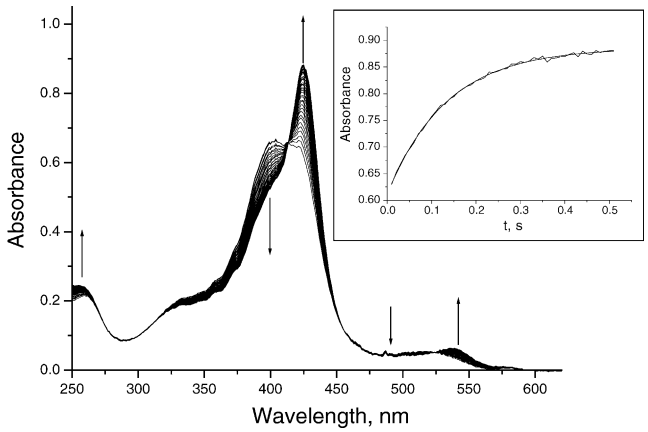

Fig. 3. Repetitive scan spectra of the reaction of $[Fe^{III}(TMPyP)(H_2O)_2]^{5+}$ with NO. $[Fe^{III}(TMPyP)(H_2O)_2{}^{5+}] = 1 \times 10^{-5}$ M, [NO] = 0.7 mM, pH = 1, μ = 0.1 M and temperature = 25 °C. The spectra were recorded every 20 ms. (Inset) Kinetic trace at 424 nm fitted with a single exponential function. The points were extracted from spectra recorded at a time interval of 10 ms.

to follow pseudo-first-order kinetics in the presence of an excess NO, for which the observed rate constant can be expressed by

$$k_{obs} = k_{on}[NO] + k_{off} \quad (1)$$

Spectral changes and a typical kinetic trace at 424 nm are shown in Fig. 3. Only a single exponential reaction step was observed at pH = 1. The plot of k_{obs} versus [NO] should be linear with a slope k_{on} and an intercept k_{off}. In general, the extrapolation of the kinetic data to [NO] = 0 does not allow an accurate determination of k_{off}, and another approach was adopted to determine k_{off} in a direct manner. The reaction was found not go to completion, such that a mixture of $[Fe^{III}(TMPyP)(H_2O)_2]^{5+}$, $[Fe^{II}(TMPyP)(NO)^{+}]^{5+}$ and NO remains at the end of the reaction.

The large absorbance changes in the Soret band that accompany the reaction with NO (Fig. 3) are characteristic for an electron transfer process since the iron center of the porphyrin complex is formally reduced to Fe(II), i.e. resulting in a d^6 electronic structure. This is characteristic for the Fe^{II}–NO^{+} nature of the nitrosylation product.

The NO concentration dependence of the nitrosylation reaction was studied as a function of temperature in the range 5–20 °C. As shown in Fig. 4, a linear dependence of k_{obs} on the NO concentration was obtained. From the slope of the lines the second-order rate constant k_{on} was calculated as a function of temperature (see Table 1). The thermal activation parameters were determined from an Eyring plot (see Figure S1, Supporting Information), and resulted in $\Delta H^{\neq} = 67 \pm 4$ kJ mol^{-1} and $\Delta S^{\neq} = +67 \pm 13$ J mol^{-1} K^{-1}.

The rate constant for the "off" reaction was calculated from the intercepts of the plots in Fig. 4 (see Table 1). From the values of k_{off} as a function of temperature, the thermal activation parameters were determined from an Eyring plot (see Figure S2) and found to be $\Delta H^{\neq} = 108 \pm 5$ kJ mol^{-1} and $\Delta S^{\neq} = 150 \pm 12$ J mol^{-1} K^{-1}. In order to check the correctness of the values of k_{off}, another procedure was adopted. The hexaaqua-iron(II) complex reacts very fast with NO ($k_{on} = 1.42 \times 10^6$ M^{-1} s^{-1} at 25 °C) [21], and can therefore be used as NO scavenger. Since the release of NO from the nitrosyl complex is slow, it is possible to follow the kinetics of the release of NO by addition of aquated iron(II). The free NO in solution rapidly binds to $[Fe(H_2O)_6]^{2+}$ within the mixing time of the stopped-flow instrument, which is followed by a slow reaction that is controlled by the release of NO from the nitrosyl complex as shown in Scheme 3 (aquated Fe(II) is used in at least a 20-fold excess with respect to the porphyrin complex). The rate of the reaction only depends on the release of NO, since k_{bind} is very

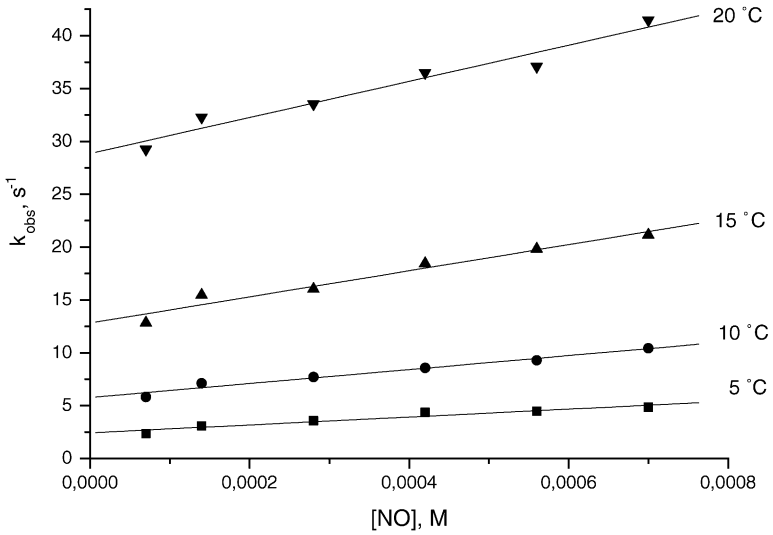

Fig. 4. Concentration dependence of k_{obs} for the reaction of $[Fe^{III}(TMPyP)(H_2O)_2]^{5+}$ with NO as a function of temperature. $[Fe^{III}(TMPyP)(H_2O)_2{}^{5+}] = 1 \times 10^{-5}$ M, pH = 1, μ = 0.1 M.

Table 1
Rate constants and activation parameters for the "on" and "off" reactions for the reversible binding of NO to $[Fe^{III}(TMPyP)(H_2O)_2]^{5+}$

T (°C)	"On" reaction		"Off" reaction	
	P (MPa)	$k_{on} \times 10^{-3}$ ($M^{-1}\,s^{-1}$)[a]	k_{off} (s^{-1})[a]	k_{off} (s^{-1})[b]
5.0	0.1	3.7 ± 0.5	2.4 ± 0.2	2.3 ± 0.3
10.0	0.1	6.6 ± 0.6	5.8 ± 0.2	6.4 ± 0.6
15.0	0.1	12.4 ± 1.3	12.8 ± 0.5	14.6 ± 1.0
20.0	0.1	17 ± 2	28.8 ± 0.8	29.9 ± 0.9
25.0	0.1	29 ± 2[c]	59 ± 4[c]	66 ± 6[c]
5.0	10	4.2 ± 0.1	–	4.0 ± 0.3
	50	4.4 ± 0.2	–	3.0 ± 0.1
	90	4.8 ± 0.2	–	2.3 ± 0.1
	130	5.1 ± 0.2	–	1.7 ± 0.2
$\Delta H^{\neq}$ (kJ mol^{-1})		67 ± 4	108 ± 5	113 ± 5
$\Delta S^{\neq}$ (J $mol^{-1}\,K^{-1}$)		$+67 \pm 13$	$+150 \pm 12$	$+169 \pm 18$
$\Delta V^{\neq}$ ($cm^3\,mol^{-1}$)		$+3.9 \pm 1.0$	–	$+16.6 \pm 0.2$

The rates at 25 °C were not determined experimentally but extrapolated from the Eyring plots to 25 °C.
[a] Determined from the slope and intercept of the plots shown in Fig. 4.
[b] Determined directly using Fe_{aq}^{2+} to scavenge NO from an equilibrium mixture.
[c] Calculated from the extrapolation of the Eyring plots at 25 °C.

fast as mentioned above. Variation of the $[Fe^{II}(H_2O)_6^{2+}]$ or the porphyrin concentration had no effect on the observed rate constant, indicating that the release of NO is the rate-determining step under the selected conditions. The values of k_{off} determined in this way are in good agreement with those calculated from the intercepts of the plots in Fig. 4 and are included in Table 1. These values can also be used to determine the activation parameters for the release of NO (see Figure S3), viz. $\Delta H^{\neq} = 113 \pm 5\,kJ\,mol^{-1}$ and $\Delta S^{\neq} = 169 \pm 18\,J\,mol^{-1}\,K^{-1}$.

The pressure dependence of the "on" and "off" reactions was also studied. Before the measurements were performed in the high-pressure stopped-flow, the syringes of the instrument were flashed with argon-saturated water to ensure the absence of traces of oxygen during the measurements. The slopes of the dependence of k_{obs} on the concentration of NO as a function of pressure (see Figure S4) were used to calculate the activation volume for k_{on} according to Eq. (2) (see Figure S5):

$$\Delta V^{\neq} = -RT\left[\frac{\mathrm{d}\ln k_i}{\mathrm{d}P}\right]_T \quad (2)$$

The activation volume for the release of NO (k_{off}) was measured directly by following the reaction of the nitrosyl complex with $[Fe^{II}(H_2O)_6]^{2+}$ as a function of pressure. For the "on" reaction the activation volume was found to be $+3.9 \pm 1.0\,cm^3\,mol^{-1}$. This value is much smaller than the value found for the release of NO from the nitrosyl complex, viz. $+16.6 \pm 0.2\,cm^3\,mol^{-1}$. From these activation volume data it was possible to construct the volume profile for the overall reaction shown in Fig. 5. All the rate and activation parameters for the reversible binding of NO are summarized in Table 1.

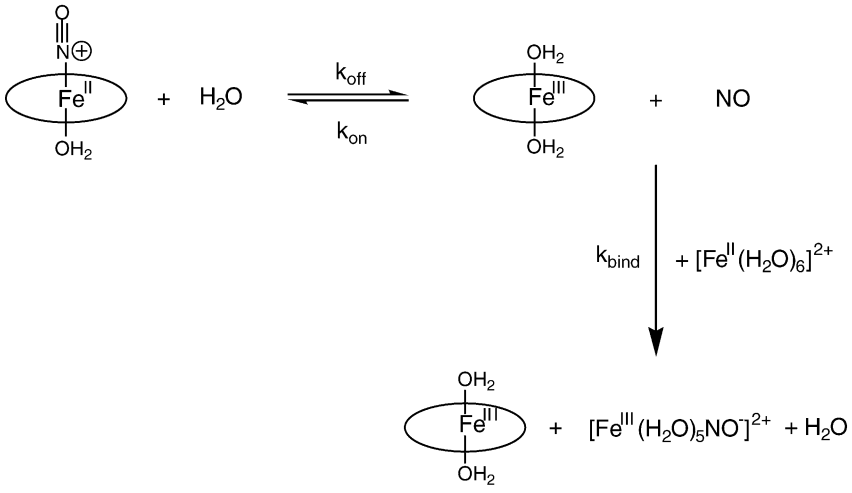

Scheme 3. Determination of the rate constant for the release of NO from the nitrosyl complex. The observed rate constant equals k_{off} and was determined from the single exponential fit of the kinetic trace at 451 nm.

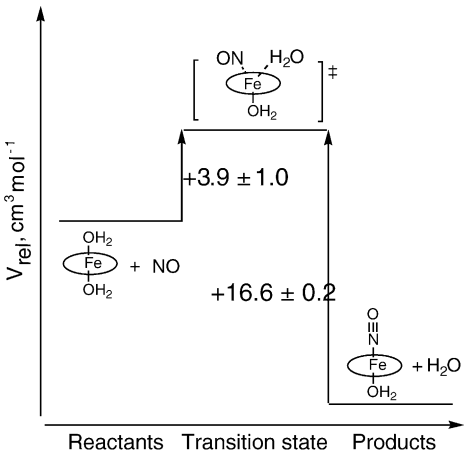

Fig. 5. Volume profile for the overall reaction in Scheme 2.

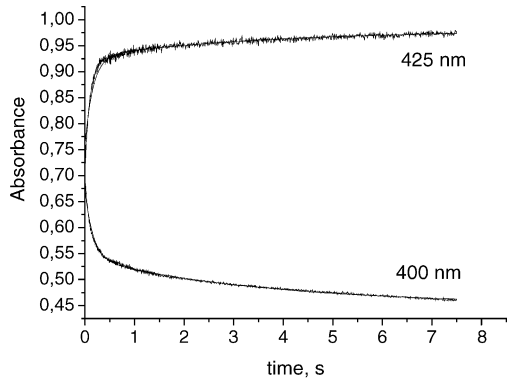

Fig. 6. Kinetic trace with a two-exponential fit at 400 and 425 nm.

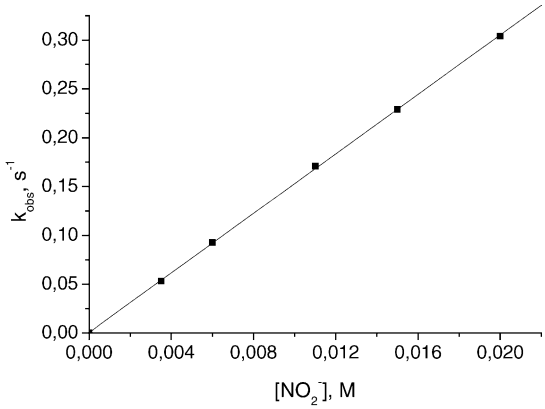

Fig. 7. Nitrite concentration dependence of the reaction of $[Fe^{II}(TMPyP)(H_2O)(NO^+)]^{5+}$ with NO_2^-. $[Fe^{II}(TMPyP)(H_2O)(NO^+)^{5+}] = 1 \times 10^{-5}$ M, pH = 4, μ = 0.1 M, temperature = 15 °C.

3.2. UV–vis observations and kinetics of the reaction of NO_2^- with $[Fe^{II}(TMPyP)(H_2O)(NO^+)]^{5+}$

When the reaction of NO with $[Fe^{III}(TMPyP)(H_2O)_2)]^{5+}$ is studied in aqueous solution at pH > 3, a second slower reaction is observed. This led us to consider the possible role of nitrite in this reaction. When the reaction is studied in at least a 10-fold excess of nitrite, the kinetic trace can be fitted with a two-exponential fit as shown in Fig. 6. The first reaction step is fast and in agreement with the reaction of the diaqua complex with NO as reported in the previous section. The subsequent reaction depends linearly on the nitrite concentration as shown in Fig. 7. The product of the reaction was identified as $[Fe^{II}(TMPyP)(H_2O)(NO^{\bullet})]^{4+}$, since the final spectrum is identical to the one obtained on addition of NO to the reduced $[Fe^{II}(TMPyP)(H_2O)_2]^{4+}$ complex. Addition of nitrite to this complex did not have any effect on the position of the Soret band at 425 nm. In this case the reaction takes place as suggested in Scheme 4. For this mechanism, the observed pseudo-first-order rate constant should follow the rate law given in Eq. (3), where k_{nit} represents the rate constant for the reaction of $[Fe^{II}(TMPyP)(H_2O)(NO^+)]^{5+}$ with nitrite:

$$k_{obs} = \frac{k_{nit} K_{NO}[NO][NO_2^-]}{1 + K_{NO}[NO]} \quad (3)$$

Thus the slope of the line in Fig. 7, viz. $15.23 \pm 0.09\ M^{-1}\ s^{-1}$ at 15 °C, represents $k_{nit}K_{NO}[NO]/(1 + K_{NO}[NO])$, from which the value of k_{nit} can be calculated since K_{NO} and [NO] are in principle known under all experimental conditions. From the

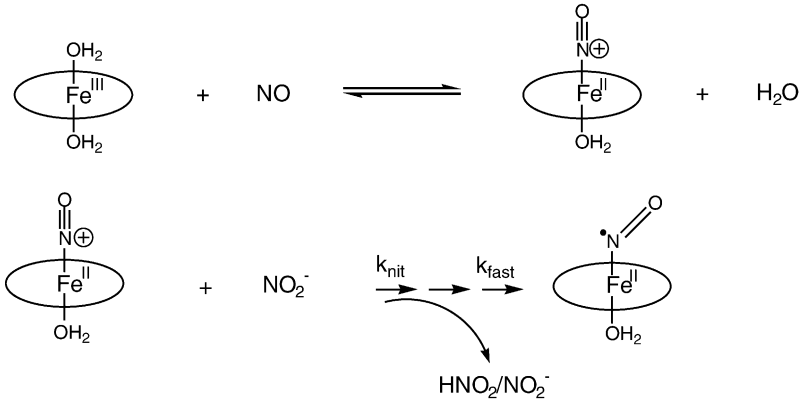

Scheme 4. Suggested steps for the reaction of $[Fe^{II}(TMPyP)(H_2O)(NO^+)]$ with nitrite.

Table 2
Values of K_{NO} as a function of temperature and pressure

Temperature (°C)	Pressure (MPa)	K_{NO} (M^{-1})
5.0	0.1	1610 ± 302
10.0	0.1	1031 ± 135
15.0	0.1	849 ± 106
20.0	0.1	575 ± 69
25.0	0.1	439 ± 50
30.0	0.1	322 ± 42
35.0	0.1	242 ± 32
40.0	0.1	184 ± 24
15.0	10	897 ± 108
	50	1112 ± 116
	90	1380 ± 28
	130	1712 ± 142

temperature and pressure dependence of k_{on} and k_{off} for the reversible formation of $[Fe^{II}(TMPyP)(H_2O)(NO^+)]^{5+}$, K_{NO} ($=k_{on}/k_{off}$) was calculated (Figure S6) and the results are summarized in Table 2. The values for K_{NO} as a function of pressure at 15 °C were calculated from the value of K_{NO} at ambient pressure and the reaction volume $\Delta V(K_{NO}) = \Delta V^{\neq}_{on} - \Delta V^{\neq}_{off}$ determined at 5 °C, where the high-pressure kinetic data for the "on" and "off" reactions was measured. It is generally known that activation volumes are not very temperature sensitive, such that this small temperature difference will not affect the treatment of the data.

The values of k_{nit} as a function of temperature and pressure are listed in Table 3. From the linear Eyring plot for this data (see Figure S7), the thermal activation parameters $\Delta H^{\neq} = 88 \pm 2\,kJ\,mol^{-1}$ and $\Delta S^{\neq} = +92 \pm 6\,J\,mol^{-1}\,K^{-1}$ were obtained. From the linear plot of $\ln(k_{nit})$ versus pressure (see Figure S8), $\Delta V^{\neq}$ was calculated to be $+8.8 \pm 0.1\,cm^3\,mol^{-1}$.

3.3. Mechanistic interpretation

It is clear from the activation parameters in Table 1, that the substitution of a coordinated water molecule by NO follows a dissociative interchange (I_d) mechanism. The volume profile in Fig. 5 demonstrates the dissociative character of the transition state. By way of comparison with the data for the other investigated porphyrin complexes (summarized in Table 4), the reaction of $[Fe^{III}(TMPyP)(H_2O)_2]^{5+}$ with NO is between 25 and 100 times slower than the reaction with $[Fe^{III}(TPPS)(H_2O)_2]^{3-}$ and $[Fe^{III}(TMPS)(H_2O)_2]^{3-}$, respectively. Also the "off" reaction for this complex is significantly slower. This means that bond cleavage for the TMPyP system is much slower than for the TPPS and TMPS systems. This is related to the electrophilicity of the Fe center in the TMPyP complex, which is due to the large 4+ positive charge on the porphyrin, significantly higher than for the other two systems where the porphyrin carries a 4− negative charge.

Table 3
Rate and activation parameters for the reaction of $[Fe^{III}(TMPyP)(H_2O)(NO)^+]^{5+}$ with nitrite

Temperature (°C)	Pressure (MPa)	k_{obs} (s^{-1})	k_{nit} ($M^{-1}\,s^{-1}$)
5.0	0.1	0.14 ± 0.01	13.2 ± 1.7
10.0	0.1	0.19 ± 0.01	22.0 ± 1.4
15.0	0.1	0.30 ± 0.02	41 ± 3
20.0	0.1	0.47 ± 0.03	82 ± 5
25.0	0.1	0.75 ± 0.05	159 ± 12
30.0	0.1	1.13 ± 0.10	307 ± 33
35.0	0.1	1.50 ± 0.12	518 ± 57
40.0	0.1	2.16 ± 0.20	946 ± 119
15.0	10	0.2823 ± 0.02	37 ± 3
	50	0.2731 ± 0.03	31 ± 4
	90	0.2658 ± 0.02	27 ± 2
	130	0.2564 ± 0.02	23 ± 2
$\Delta H^{\neq}$ ($kJ\,mol^{-1}$)			88 ± 2
$\Delta S^{\neq}$ ($J\,mol^{-1}\,K^{-1}$)			+92 ± 6
$\Delta V^{\neq}$ ($cm^3\,mol^{-1}$)			+8.8 ± 0.1

The k_{obs} values were measured at $[NO_2^-] = 0.02$ M.

Table 4
Rate and activation parameters for the "on" and "off" reactions for the binding of NO to a series of porphyrin complexes

	$[Fe^{III}(TPPS)(H_2O)_2]^{3-} + NO$[a]		$[Fe^{III}(TMPS)(H_2O)_2]^{3-} + NO$[a]		$[Fe^{III}(TMPyP)(H_2O)_2]^{5+} + NO$[b]	
	k_{on} ($M^{-1}\,s^{-1}$)	k_{off} (s^{-1})	k_{on} ($M^{-1}\,s^{-1}$)	k_{off} (s^{-1})	k_{on} ($M^{-1}\,s^{-1}$)	k_{off} (s^{-1})
k at 25 °C	$(0.50 \pm 0.03) \times 10^6$	$(0.5 \pm 0.4) \times 10^3$	$(2.8 \pm 0.2) \times 10^6$	$(0.9 \pm 0.2) \times 10^3$	$(2.9 \pm 0.2) \times 10^4$	66 ± 6
$\Delta H^{\neq}$ ($kJ\,mol^{-1}$)	69 ± 3	76 ± 6	57 ± 3	84 ± 3	67 ± 4	113 ± 5
$\Delta S^{\neq}$ ($J\,mol^{-1}\,K^{-1}$)	+95 ± 10	+60 ± 11	+69 ± 11	+94 ± 10	+67 ± 13	+169 ± 18
$\Delta V^{\neq}$ ($cm^3\,mol^{-1}$)	+9 ± 1	+18 ± 2	+13 ± 1	+17 ± 3	+3.9 ± 1.0	+16.6 ± 0.2

[a] Data taken from Ref. [6].
[b] This work, data taken from Table 1.

The stronger Fe–OH_2 bond in $[Fe^{III}(TMPyP)(H_2O)_2]^{5+}$ is responsible for the changeover from a limiting dissociative (D) substitution mechanism in the case of the corresponding TPPS and TMPS complexes, to an I_d mechanism in which bond breakage is accompanied by partial bond-formation with the entering nucleophile. This clearly shows up in the lower activation volume found for the "on" reaction in the case of the $[Fe^{III}(TMPyP)(H_2O)_2]^{5+}$ complex. In all three systems the "off" reaction is characterized by a very similar and positive volume of activation, which is ascribed to the breakage of the Fe^{II}–NO^+ bond that is accompanied by electron transfer from Fe(II) to NO^+ to produce Fe(III) and NO. The latter process is also accompanied by a change in spin state from low spin to high spin, which is expected to be accompanied by a volume increase of between 10 and 15 $cm^3\,mol^{-1}$ [4].

By way of comparison, Table 5 summarizes the results for the water exchange reactions of $[Fe^{III}(TPPS)(H_2O)_2]^{3-}$, $[Fe^{III}(TMPS)(H_2O)_2]^{3-}$ and $[Fe^{III}(TMPyP)(H_2O)_2]^{5+}$. It is clearly seen that water exchange on $[Fe^{III}(TMPyP)(H_2O)_2]^{5+}$ is much slower than for the other two complexes [11], in line with the trend in the values of k_{on} and k_{off} in Table 4. Thus the lability of the Fe–OH_2 bond in these systems clearly controls the rate of the reversible complex-formation reactions with NO. The activation parameters for the water exchange process are in line with a limiting D or I_d mechanisms depending on the ground state labilization of the Fe–OH_2 bond, which will be determined by the electron donating/withdrawing properties of the substituted porphyrin, which in turn will depend on the anionic/cationic nature of the substituents, respectively. Thus, the water exchange process in principle controls the rate and mechanism of the nitrosylation reaction.

At low pH, where traces of nitrite (always present in aqueous solutions of NO) will be present as HONO, there is no subsequent catalytic effect of nitrite on the reductive nitrosylation reaction. However, at pH > 3 where nitrite is present in the anionic form, the experimental results clearly show that nitrite catalyzes a subsequent reaction. Nitrite reacts with $[Fe^{II}(TMPyP)(H_2O)(NO^+)]^{5+}$ to produce $[Fe^{II}(TMPyP)(H_2O)]^{4+}$ which is expected to bind NO in a diffusion-controlled step as reported for closely related Fe(II)-porphyrins (k_{on} is of the order of $10^9\,M^{-1}\,s^{-1}$) [6] to form $[Fe^{II}(TMPyP)(H_2O)NO^{\bullet}]^{4+}$ as final reaction product. Ford and co-workers have investigated this reaction for metHb and $[Fe^{III}(TPPS)(H_2O)_2]^{3-}$ [12,22], and suggested

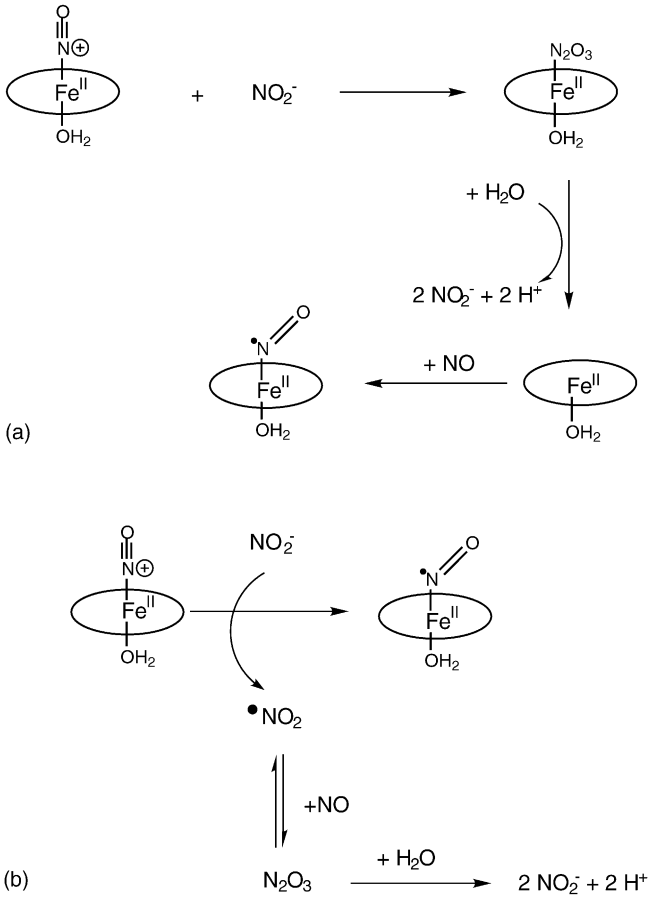

Scheme 5. Two possible reaction mechanisms that can account for the catalytic effect of nitrite during the reductive nitrosylation reaction.

two possible reaction mechanism to account for the catalytic effect of nitrite. The first one (Scheme 5a) involves the nucleophilic attack of nitrite on the electrophilic, positively charged, coordinated NO^+, to produce N_2O_3 which is the anhydride of nitrous acid. This molecule rapidly reacts with water to produce nitrite and H^+ ions. Subsequently, penta-coordinate $[Fe^{II}(TMPyP)(H_2O)]^{4+}$ rapidly reacts with NO to produce the final $[Fe^{II}(TMPyP)(H_2O)NO^{\bullet}]^{4+}$ product. The second reaction sequence (Scheme 5b) involves an outer-sphere electron transfer process between nitrite and coordinated NO^+ to form $[Fe^{II}(TMPyP)(H_2O)NO^{\bullet}]^{4+}$. The produced NO_2 radical then rapidly reacts with NO to produce N_2O_3, which immediately reacts with water to produce two molecules of nitrous acid, or two ni-

Table 5
Rate and activation parameters for water-exchange reactions on a series of iron(III) porphyrin complexes [11]

	k_{ex}[a] (s^{-1})	$\Delta H^{\neq}$ ($kJ\,mol^{-1}$)	$\Delta S^{\neq}$ ($J\,K^{-1}\,mol^{-1}$)	$\Delta V^{\neq}$ ($cm^3\,mol^{-1}$)
$[Fe(TPPS)(H_2O)_2]^{3-}$	$(2.0 \pm 0.1) \times 10^6$	67 ± 2	99 ± 10	$+7.9 \pm 0.2$
$[Fe(TMPS)(H_2O)_2]^{3-}$	$(2.1 \pm 0.1) \times 10^7$	61 ± 1	100 ± 5	$+11.9 \pm 0.3$
$[Fe(TMPyP)(H_2O)_2]^{5+}$	$(4.5 \pm 0.1) \times 10^5$	71 ± 2	100 ± 6	$+7.4 \pm 0.4$

[a] Temperature: 25 °C.

trite ions and two protons depending on the pH of the solution.

Our kinetic data show that the subsequent catalytic reaction exhibits a linear dependence on the nitrite concentration. In addition the activation parameters, especially the activation entropy and activation volume for this process are significantly positive (see Table 3). This can be related to the fact that the binding of nitrite to coordinated NO^+, or the outer-sphere reduction of coordinated NO^+ by nitrite, is accompanied by charge neutralization which is accompanied by a decrease in electrostriction, i.e. release of solvent molecules and an increase in both the entropy and molar volume in the transition state. Electrostriction effects can in certain cases overrule intrinsic effects and cause the overall volume of activation to be positive even for a bond-formation process as suggested in Scheme 5a, i.e. the negative contribution from $\Delta V^{\neq}_{\text{intr}}$ is significantly smaller than the positive contribution from $\Delta V^{\neq}_{\text{solv}}$ [23]. On the basis of these activation parameters it is presently not possible to distinguish between the two possible reaction mechanisms outlined in Scheme 5. Further experiments are presently under consideration in order to distinguish between the two possible reaction mechanisms.

Acknowledgements

The authors gratefully acknowledge financial support from the Max-Buchner Forschungsstiftung, the Deutsche Forschungsgemeinschaft as part of SFB 583 “Redox-Active Metal Complexes” and the European Community Project No. MRTN-CT-2003-50386 (AQUACHEM).

Appendix A. Supplementary data

Supplementary data associated with this article can be found, in the online version, at 10.1016/j.molcata.2004.09.021.

References

[1] A. Friebe, D. Koesling, Circ. Res. 31 (2003) 2010.
[2] P. Nicholis, M. Sharpe, J. Torres, M.T. Wilson, C.E. Cooper, Biochem. Soc. Trans. 26 (1998) 323.
[3] A. Wanat, J. Gdula-Arganiska, D. Rutkotwa-Zbik, M. Witko, G. Stochel, R. van Eldik, J. Biol. Inorg. Chem. 7 (2002) 165.
[4] M. Hoshino, L. Laverman, P.C. Ford, Coord. Chem. Rev. 187 (1999) 75.
[5] A. Franke, C. Jung, R. van Eldik, J. Am. Chem. Soc. 126 (2004) 4181.
[6] L.E. Laverman, P.C. Ford, J. Am. Chem. Soc. 123 (2001) 11614.
[7] T. Schneppensieper, A. Wanat, G. Stochel, S. Goldstein, D. Meyerstein, R. van Eldik, Eur. J. Inorg. Chem. (2001) 2317.
[8] E.B. Fleisher, D.A. Fine, Inorg. Chim. Acta 29 (1978) 267.
[9] J. Chen, O. Ikeda, T. Hatasha, A. Kitajama, M. Miyake, A. Yamatodani, Electrochem. Commun. 1 (1999) 274.
[10] M.H. Barley, K.J. Takeuchi, T.J. Meyer, J. Am. Chem. Soc. 108 (1985) 5876.
[11] T. Schneppensieper, A. Zahl, R. van Eldik, Angew. Chem. Int. Ed. 40 (2001) 1678.
[12] B.O. Fernandez, P.C. Ford, J. Am. Chem. Soc. 125 (2003) 10510.
[13] R. van Eldik, D.A. Palmer, R. Schmidt, H. Kelm, Inorg. Chim. Acta 50 (1981) 131.
[14] R. van Eldik, W. Gaede, S. Wieland, J. Kraft, M. Spitzer, D.A. Palmer, Rev. Sci. Instrum. 64 (1993) 1355.
[15] G.A. Tondreau, R.G. Wilkins, Inorg. Chem. 25 (1986) 2745.
[16] H. Kurihara, F. Arifuku, I. Ando, M. Saita, R. Nirhino, K. Ujimoto, Bull. Chem. Soc. Jpn. 55 (1982) 3515.
[17] N. Kobayashi, M. Koshiyama, T. Osa, T. Kuwana, Inorg. Chem. 22 (1983) 3608.
[18] N. Kobayashi, Inorg. Chem. 24 (1985) 3324.
[19] V.E. Yushmanov, H. Imasato, T.T. Tominaga, M. Tabak, J. Inorg. Biochem. 61 (1996) 233.
[20] L.E. Laverman, Investigations of bond making and bond breaking processes in metal nitrosyl and carbonyl porphyrins, PhD Thesis, University of California, Santa Barbara, 1999, pp. 94–95.
[21] A. Wanat, T. Schneppensieper, G. Stochel, R. van Eldik, E. Bill, K. Wieghardt, Inorg. Chem. 41 (2002) 4.
[22] B.O. Fernandez, I.M. Lorkovic, P.C. Ford, Inorg. Chem. 42 (2003) 2.
[23] R. van Eldik, F.-G. Klärner (Eds.), High Pressure Chemistry: Synthetic, Mechanistic and Supercritical Applications, Wiley/VCH, Weinheim, 2002, pp. 44–45.